The effect of fluorine doping on the properties of SnO$_2$ thin films deposited using spray pyrolysis method

YOUSSEF LARBAH[a,*], BADIS RAHAL[a], MOHAMED ADNANE[b]

[a]*Spectrometry Department, Nuclear Research Center of Algiers-CRNA 02 Bd. Frantz Fanon BP 399 Algiers, Algeria*
[b]*Technology Department, University of Science and Technology of Oran. USTO-MB, B.P. 1505, 31000 El-Mnaouer Oran, Algeria*

In this paper, we report on the structural and optical properties of undoped and fluorine-doped tin oxide (SnO$_2$:F) thin films deposited by spray pyrolysis at 400°C. The XRD analysis indicates that all films present tetragonal rutile structure with a preferred orientation changes from (110) to (211). The average grain size is about 50 nm, and decreases with the incorporation of Fluorine. The scanning electron microscopy (SEM) analyses have shown that nanoparticles size to 78 nm. The films exhibit a high transmittance 85%. The optical gap varies from 3.97 to 4eV. The electrical study reveals that the films exhibit n-type conductivity with the lowest value of resistance layer, of 13(Ω/γ) for films doped with 9.wt% F.

3. Introduction

Transparent conducting oxide (TCO) thin films have important applications in the optoelectronics due to their optical and electrical properties [1-2]. Among these oxides, indium tin oxide (ITO) this oxide poses problems particularly it is rare and high cost. There are many studies to replace the ITO with oxide present high optical transparency, high chemical stability, and at low cost. The undoped and fluorine-doped tin oxide (SnO$_2$:F) is one of the TCO to replace the ITO because the high optical transparency in the visible spectrum, high chemical stability, and low sheet resistance. The advantage of SnO$_2$ thin films is the fact that its component are non-toxic. Fluorine-doped tin oxide (SnO$_2$:F) is an excellent transparent used in optoelectronic devices [3-5]. Fluorine-doped tin oxide deposition can be carried out by different methods, such as chemical vapor deposition [6, 7], Sol-Gel [8, 9] and spray pyrolysis [10-14]. The latter technique is simple and applicable to large area depositions, the deposition can be carried out at atmospheric pressure. In the present work F-doped SnO$_2$ thin films were prepared by spray pyrolysis technique on glass substrates. The purpose of this work is to study the effect of the doping concentration on some physical properties of SnO$_2$:F thin films such as crystal structure, surface morphology, optical and electrical properties. The results obtained are compared and discussed with the specified results by some researchers.

2. Experimental

Thin films of undoped and fluorine-doped tin oxide (SnO$_2$-F) were deposited on optical glass substrate by homemade spray pyrolysis technique [14,16]. Tin chloride ehydrate (SnCl$_2$.2H$_2$O) was used as the source for tin; 0.4 M of SnCl$_2$.2H$_2$O dissolved in mixture of methanol and distilled water served as starting solution. The doping was achieved by the addition of ammonium fluoride (NH$_4$F) to the spraying solution, and the whole mixture was sprayed onto microscopic glass slides. The optimal substrate temperature was obtained from the work of Labrah and al [15]. We selected the temperature of 400°C for all samples following. The deposition time was 10 minutes for all the depositions. The fluorine doping concentration was varied from 0 to 15.wt% in the spray solution. The carrier gas flow rate was maintained at 10 l/min. The normalized distance between the spray nozzle and the substrate is 27 cm. The spray time interval was at 20 s, the flow rate of the spray solution is 15ml/h [15]. The structural properties of the prepared films were analyzed by a Siemens diffractometer, with using CuKα radiation at 40 kV and 30 mA. Samples were observed by scanning electron microscope using a Philips XL30 Field-Emission (ESEM-FEG) and the composition chemical were obtained using the EDX (Energy dispersive spectrometers). The optical measurements of undoped and F-doped SnO$_2$ films were carried out at room temperature using UV-VIS spectrophotometer in the wavelength range of 300 –1100 nm.

3. Results and discussion

3.1. Structure

The X-ray diffraction patterns of SnO₂ and SnO₂: F films are shown as Fig. 1. All the films are found to have tetragonal rutile structure with a polycrystalline nature [15, 16]. All the patterns contain the characteristic SnO₂ peaks only. The un-doped SnO₂ film shows a preferred orientation along plane (110), which changes into plane (211) gradually as the increase of Fluor concentration. Other orientations (200), (211), (220), (310) and (301) are also observed, but with lower intensities. The presence of other phase such as (SnF₂) is detected, indicating the (O) atoms were replaced by (F) atoms in the (SnO₂: F) films [17.18], the formation of this phase explains by the saturation of fluorine. The crystallite size is estimated by using Scherrer's formula given by equation (1).

$$D = \frac{(0.9\lambda)}{\beta \cos \theta_{(hkl)}} \qquad (1)$$

where D is the grain size of crystallite, λ (1.54059A) represents the wavelength of X-rays used, β (FWHM) is the full width at half maximum of peak and θ is the angle of diffraction. The calculated values of crystallite size are given in table 1. The average crystallinity size (D_{mean}) of SnO2:F thin films was decreased upon F doping at 0 and 3% , and then was increased at 9 and 15%.wt F. This means that F doping at low concentration decreases the defects in the SnO₂ films and improves crystallite quality, and the high concentration of F increases the defects so the crystallinity value increased it again with increasing of F doping concentrations.

The texture coefficient T $_{(hkl)}$ can be determined using the following equation [19] has been used to describe the preferred orientation.

$$T_{(hkl)} = \frac{I_{(hkl)}/I_{0(hkl)}}{\sum_N I_{(hkl)}/I_{0(hkl)}} \qquad (2)$$

where (hkl) represent the indices of the peak, T is the coefficients texture following of the (hkl) plane, I(hkl) is the measured intensity, I₀(hkl) is the JCPDS standard intensity and N is the number of peaks.

The variation of texture coefficient for SnO₂:F thin films are listed in Table 1. After this values the preferred orientation is of (110) and (211) direction. It is seen that the texture coefficient decrease with adding fluorine

atoms in the SnO₂ films in the direction 110 against an increase in coefficient of texture with the addition of fluorine atoms in the second direction (211). Table 2 shows the lattice parameter values (a) and (c) calculated from the spectra obtained, determined from equation (3).

$$\frac{1}{d_{hkl}} = \sqrt{\frac{h^2+k^2}{a^2} + \frac{l^2}{c^2}} \qquad (3)$$

The lattice parameter values of SnO₂:F thin films at various fluorine doping are in good agreement with the JCPDS standard, where we note that a (Å) and c (Å) are found to change from 4.34 to 4.43 and 3.18 to 3.21 Å respectively. We note that a (Å) and c (Å) increase when the percentage of F increases this is confirmed by the decrease of crystal size. While there are a decrease in the parameter lattice values after 9% with increasing fluorine doping, this depends to shifting of the XRD-peaks.
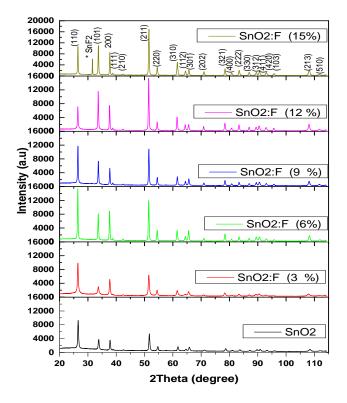

Fig. 1. X-ray diffraction patterns of undoped and F doped SnO₂ thin films (color online)

Table 1. The crystallite size and the texture coefficient of undoped and F doped SnO₂ thin films

Table 1	D (nm)				D_{mean} (nm)	T(hkl)			
	(110)	**(101)**	**(200)**	**(211)**		**(110)**	**(101)**	**(200)**	**(211)**
SnO_2	26.52	33.78	37.80	51.66	37.440	0.421	0.172	0.161	0.244
SnO_2 :F 3%	26.44	33.67	37.69	51.46	37.315	0.404	0.123	0.210	0.261
SnO_2 :F 6%	26.41	33.61	37.63	51.43	37.270	0.346	0.181	0.201	0.270
SnO_2 :F 9%	26.44	33.67	37.72	51.49	37.330	0.331	0.206	0.151	0.310
SnO_2 :F 12%	26.46	33.69	37.68	51.48	37.327	0.170	0.279	0.179	0.370
SnO_2 :F 15%	26.44	33.67	37.72	51.52	37.337	0.228	0.229	0.177	0.364

Table 2. Lattice parameter of undoped and F doped SnO₂ thin films

Fluorine Doping (%)	a (Å)	c (Å)
SnO_2	4.925	3.191
SnO_2: F 3(%)	4.935	3.201
SnO_2: F 6(%)	4.943	3.204
SnO_2: F 9(%)	4.935	3.200
SnO_2: F 12(%)	4.940	3.201
SnO_2: F 15(%)	4.934	3.199
JCPDS 00-041-1445	4.738	3.187

3.2. Scanning electron microscopy

SEM micrographs show that undoped SnO_2 and doped F 9, 12 and 15wt.% thin films has a homogeneous particles distribution. From the SEM image, we can see that the substrate is well covered with a large number of nanometric particles and the surface of the film is uniform with the average particle size about of 78 nm for all thin films (Fig. 2).

The doping of F in the film does not change the morphology of the layers. These results are in good agreement with the morphology obtained by Ian Y [20].
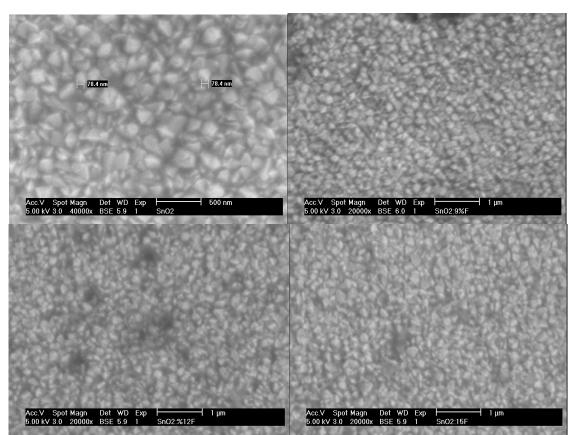

Fig. 2. SEM micrographs of SnO₂ films: (a) undoped and (b) doped F 9, 12 and 15wt.%.

3.3. Energy dispersive X-ray spectroscopy

Fig. 3 shows EDS analysis of SnO_2 thin films are nearly stoichiometric. There are no traces of other impurities like carbon etc. The EDS spectra result confirms the formation of pure SnO_2 thin films, the presence of peaks corresponding to the silicon element due to the glass substrate.
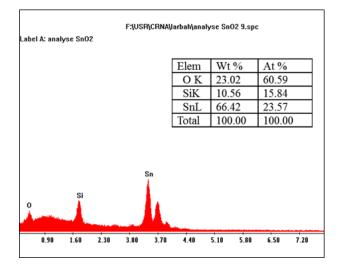
F:\USR\CRNA\larbah\analyse SnO2 9.spc

Label A: analyse SnO2

Elem	Wt %	At %
O K	23.02	60.59
SiK	10.56	15.84
SnL	66.42	23.57
Total	100.00	100.00

Fig. 3. EDS spectra of undoped SnO₂ thin films (color online)

3.4. Optical properties

The optical transmission spectrum of the SnO_2: F thin film shown in Fig. 4. The average value of transmittance of thin films in the visible range is found to be 80% - 88%, The maximum transmittance is 88% for 9 wt% F concentration [21]. In the visible region of solar spectrum, transmission spectra of SnO_2: F thin films show sinusoidal behavior that may be due to the defect formation upon F doping.

The value of band gap is estimated from fundamental absorption edge of the films. For the direct transitions, relation (4) expresses the absorption coefficient

$$\alpha = \left(ln\left(\frac{1}{T}\right) / t \right) \qquad (4)$$

Fig. 5 shows plots of $(\alpha h\nu)^2$ versus photo energy, $h\nu$, in the high absorption region. Extrapolation of the curve to $h\nu = 0$ gave the direct band gap of SnO_2: F films. The band gap varies between 3.97 eV- 4.05 eV. The values are comparable with the data already reported [22]. The band gap decreases slightly upon F doping this is explained by the introduction of donor levels in the band gap of tin oxide by fluorine consequence of effective doping. The fluorine is a better substitute for ions O^{-2} causing much more impurities. The SnO_2: F gap remains lower than that of undoped SnO_2 (4.05eV)
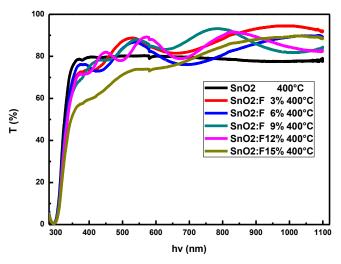
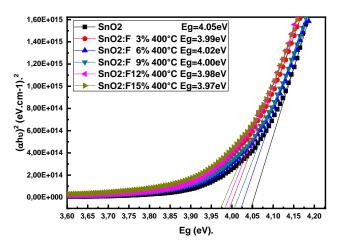*Fig. 4. Transmittance spectra of SnO₂ and different doped for flour thin films (color online)*

Fig. 5. Graph of (αhν)² versus (hν) for undoped SnO₂ and doped F 3, 6, 9, 12 and 15%wt (color online)

3.5. Sheet resistance measurements

In this part, we report on the variation of surface resistance as function of F doping concentration. The Sheet resistance (Rsh) of pure and SnO_2:F was shown in Fig.6. The Rsh of the undoped tin oxide thin films (1000 Ω /γ) decreases with increasing fluorine concentration initially and reaches a minimum value (13 Ω /γ at 9 wt.% F) afterwards increases on higher doping. This value is still high when compared to ITO. The minimum value of sheet resistance achieved in the present study is lower than those reported earlier for these films prepared from $SnCl_2$ precursor. When fluorine is incorporated in tin oxide films, each F⁻ anion substitutes an O^{2-} anion in the lattice and the substituted O^{2-} anion introduces more free electrons [23.24]. This results in an increase in free electrons and decreases the value of Rsh. This can be attributed as the reason for decreasing Rsh with increasing fluorine doping. The increase in the value of Rsh beyond a certain doping concentration of fluorine probably represents a solubility limit of fluorine in the tin oxide

lattice. The solubility limit of the fluorine in the crystal lattice is clearly seen in XRD at 15wt.% by the formation of the SnF2 phase (saturation).
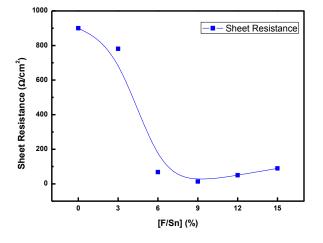

Fig. 6. Variation of sheet resistance for undoped and F-doped SnO₂ thin films (color online)

4. Conclusions

SnO_2:F thin films were prepared using spray pyrolysis method. The XRD result shows that the fluorine doped SnO_2 thin films are polycrystalline with the preferred orientation is (110) and (211). The study of the morphology by SEM confirms the nanometric nature of SnO_2 films and shows that particle size is above to 78 nm. The minimum sheet resistance values of 13 ($\Omega/\square$) as obtained for the samples with 9wt%.F, prepared from $SnCl_2$ precursor was obtained. The optical transmittance in the visible range and the optical band gap are 80% and 4 eV respectively. This simplified spray technique may be considered as a promising alternative to conventional spray for the massive production of economic SnO_2 films for solar cells.

References

[1] Arturo Morales-Acevedo, Solar Energy **80**, 675 (2006).
[2] F. de Moure-Flores, A. Guillen-Cervantes, K. E. Nieto-Zepeda, J.G. Quinones-Galvan, A. Hernandez-Hernandez, M. de la L. Olvera, M. Melendez-Lira, Revista Mexicana de Fısica **59**, 335 (2013).
[3] K. L. Chopra, S. Major, D. K. Pandya, Thin Solid Films **102**, 1 (1983).
[4] M. Turrion, J. Bisquert, P. Salvador, J. Phys. Chem. B **107**(35), 9397 (2003).
[5] M. A. Olopade, O. E. Awe, A. M. Awobode, N. Alu, The African Review of Physics **7**, 177 (2012).
[6] Te-Hua Fang, Win-Jin Chang, Applied Surface Science **252**, 1863 (2005).
[7] Qian Gao, Qiying Liu, Ming Li, Xiang Li, Yong Liu, Chenlu Song, Jianxun Wang, Junbo Liu, Ge Shen, Gaorong Han, Thin Solid Films **544**, 357 (2013).
[8] A. Banerjee, S. Kundoo, P. Saha, K. Chattopadhyay, Journal of Sol-Gel Science and Technology **28**(1), 105 (2003).
[9] Ian Y.Y. Bu, Ceramics International **40**, 417 (2014).
[10] Kodigala Subba Ramaiah, V. Sundara Raja, Applied Surface Science **253**, 1451 (2006).
[11] Hyuncheol Kim, Hyung-Ho Park, Ceramics International **38**, S609 (2012).
[12] Yang Ren, Gaoyang Zhao, Yuanqing Chen, Applied Surface Science **258**, 914 (2011).
[13] E. Elangovan, K. Ramamurthi, Thin Solid Films **476**, 231 (2005).
[14] Y. Larbah, M. Adnane, T. Sahraoui, Materials Science-Poland **33**(3), 491 (2015).
[15] Y. Larbah, M. Adnane, A. Djelloul, M. Melouki, Journal of Nano- and Electronic Physics **7**, 3013-1 (2015).
[16] Supriyono, Hedi Surahman, Yuni Krisyuningsih Krisnandi, Jarnuzi Gunlazuardi, Procedia Environmental Sciences **28**, 242 (2015).
[17] D. W. Sheel, H .M. Yates, P. Evans, U. Dagkaldiran, A. Gordijn, F. Finger, Z. Remes, M. Vanecek, Thin Solid Films **517**, 3061 (2009).
[18] Yang Ren, Gaoyang Zhao, Yuanqing Chen, Applied Surface Science **258**, 914 (2011).
[19] S. A Nasser, H. H Afify, S. A. El-Hakim, M. K. Zayed, Thin Solid Films **315**, 327 (1998).
[20] Ian Y.Y. Bu, Ceramics International **40**, 417 (2014).
[21] Qian Gao, Hong Jiang, Changjiu Li, Yanping Ma, Xiang Li, Zhaohui Ren, Yong Liu, Chenlu Song, Gaorong Han, Journal of Alloys and Compounds, **574**, 427 (2013)
[22] M. T. Mohammad, Solar Energy Mater. **20**, 297 (1990).
[23] B. Thangaraju, Thin Solid Films **402**, 71 (2002).
[24] A. A. Yadav, E. U. Masumdar, A. V. Moholkar, M. Neumann-Spallart, K. Y. Rajpure, C. H. Bhosale, Journal of Alloys and Compounds **488**, 350 (2009).

* Corresponding author: larbahyoussef@gmail.com